

RAPID COMMUNICATION

## Synthesis of graphitic carbon from *Pisum sativum* for supercapacitor applications

Pranoti H. Patil\*, Suchitra B. Ravan\*, Saurabh S. Thoravat\*, Tukaram D. Dongale\*\*,  
and Sushilkumar A. Jadhav\*<sup>†</sup>

\*School of Nanoscience and Technology, Shivaji University, Kolhapur 416004, Maharashtra, India

\*\*Computational Electronics and Nanoscience Research Laboratory, School of Nanoscience and Technology,  
Shivaji University, Kolhapur 416004, Maharashtra, India

(Received 19 April 2023 • Revised 30 May 2023 • Accepted 29 June 2023)

**Abstract**—This work reports preparation of *Pisum sativum* (peas) derived graphitic carbon (PSC) and its activation with potassium hydroxide (KOH), referred to as *Pisum sativum* derived activated graphitic carbon (PSAC). The structure, morphology and surface area of the materials were characterized by using X-ray diffraction (XRD) analysis, Fourier transform infrared spectroscopy (FTIR), scanning electron microscopy (SEM), Raman spectroscopy and Brunauer Emmet Teller (BET). The electrochemical performance of the material was investigated by using cyclic voltammetry (CV), galvanostatic charge-discharge (GCD), cyclic stability and electrochemical impedance spectroscopy (EIS). The graphitic carbon obtained showed specific surface area of  $240 \text{ m}^2 \text{ g}^{-1}$  with pore size of 3.32 nm. The electrochemical testing of activated carbon delivered specific capacitance of  $517 \text{ F g}^{-1}$  at  $10 \text{ mV s}^{-1}$  with 86% of capacitance retention after 2,000 cycles at  $10 \text{ mA cm}^{-2}$ . It showed high specific energy of  $35 \text{ Wh kg}^{-1}$  at specific power  $645 \text{ W kg}^{-1}$ .

Keywords: *Pisum sativum*, Carbon Materials, Graphitic Carbon, Thin Films, Electrical Properties

### INTRODUCTION

The development of efficient energy storage systems is essential for storing energy. Among the various energy storage devices, supercapacitors (SCs) have piqued the interest of researchers due to their unique characteristics, such as high storage capacity, rapid charging-discharging, higher power density, long retention time and environmental friendliness [1,2]. Despite having high power density, SCs are not able to reach high energy density requirements, particularly for use in electric vehicles [3]. Intensive research is being carried out for the development of new electrode materials for SCs [4]. SCs are mainly classified into three types: electric double layer capacitors (EDLC), pseudo capacitor and hybrid [5]. Carbon is commonly used in electric double layer capacitors (EDLC) because of its high abundance, low cost, easy synthesis and excellent properties like good conductivity, high stability, and easy surface modification [6,7]. Many carbon materials with high specific surface areas (SSAs) are prepared from high-cost and unsustainable chemical petroleum resources, leading to side effects for the environment [8]. The synthesis of graphitic carbons by green route or by using naturally abundant materials as source of carbon makes the process economical [9].

To overcome this problem, biomass or natural resources with low cost and easy availability are investigated as an alternative for obtaining high value carbon [10-12]. Among many kinds of materials, the use of some food materials, such as peas (*Pisum sativum*), can also yield good quality carbon upon carbonization under controlled atmospheres. This will reveal the additional value of vegetable food

stuffs for the preparation of high-quality carbon [13]. Therefore, this work is focused on preparation of high-quality graphitic carbon from peas (referred to as PSC), its activation with KOH, referred to as *Pisum sativum* activated carbon (PSAC), and testing of its electrochemical performance for supercapacitive application. The results revealed a good quality carbon with superior performance can be obtained, thus making the finding a significant advancement in the field of EDLCs.

### EXPERIMENTAL

#### 1. Materials and Instruments

These details are given in the ESI.

#### 2. Synthesis of PSC and PSAC Materials

##### 2-1. Preparation of PSC

Dry peas were washed with deionized water and dried in an oven. The dried peas were ground to make fine powder and pyrolyzed at  $800 \text{ }^\circ\text{C}$  under  $\text{N}_2$  atmosphere in a tubular furnace for 2 h. After carbonization, the size of prepared carbon material was reduced by ball milling the sample in a planetary ball mill for 3 h.

##### 2-2. Preparation of PSAC

PSC was activated with KOH with a ratio of 4:1 (KOH:PSC). The mixtures were impregnated and stirred with 40 ml ethanol to make a paste. After soaking at room temperature for 12 h, the paste was completely dried. The dried mass was heated at  $800 \text{ }^\circ\text{C}$  under  $\text{N}_2$  atmosphere in a tubular furnace for 2 h. The activated sample was washed with distilled water and dried in an oven at  $70 \text{ }^\circ\text{C}$  for 24 h.

##### 2-3. Electrochemical Measurements

The electrochemical experiments were carried out by using a 3-electrode assembly in a 1 M KOH electrolyte. The electrode was prepared by mixing sample, carbon black and polyvinylidene fluo-

<sup>†</sup>To whom correspondence should be addressed.

E-mail: sushil.unige@gmail.com

Copyright by The Korean Institute of Chemical Engineers.

ride (PVDF) binder (8 : 1 : 1) proportion in *N*-methyl pyrrolidone (NMP) solvent.

## RESULTS AND DISCUSSION

### 1. X-ray Diffraction (XRD)

The XRD was used to analyze the structural properties of the synthesized samples. Fig. 1(A) shows the XRD patterns of the synthesized PSC and PSAC samples. The XRD pattern for the sample PSC displays two small broad diffraction peaks around  $23.9^\circ$  and  $43.4^\circ$  corresponding to the (002) and (100) diffractions for graphitic carbon. The XRD pattern for sample PSAC shows diffraction peaks located at  $2\theta = 23.9^\circ$  and another peak at  $2\theta = 43.4^\circ$ , which are sharper than PSC diffraction peaks. According to these peaks, it is possible that the activated carbon contains potassium with high crystallinity after being activated with KOH. The broad and weak peaks in this XRD pattern indicate the amorphous nature of carbon. Their appearance illustrates the existence of micro-graphitic structure in PSC and PSAC samples [14,15].

### 2. Raman Spectroscopy

The graphitization degree and defects were confirmed by Raman spectroscopy. Fig. 1(B) shows the Raman spectra of the synthesized PSC and PSAC samples. The peaks observed at  $1,351\text{ cm}^{-1}$  and  $1,349\text{ cm}^{-1}$  in the PSC and PSAC samples, respectively, are referred to as D band and the peaks at  $1,590\text{ cm}^{-1}$  and  $1,600\text{ cm}^{-1}$  in the PSC and PSAC samples, respectively, are referred to as G

band. The D band presents a favorable situation for charge storage, while the G band is good for electrical conductivity. The calculated intensity ratio of PSC and PSAC of D to G band ( $I_D/I_G$ ) was found to be 1.17 and 1.18, respectively [16,17].

### 3. Infrared Spectroscopy (FTIR)

Structural information of the synthesized samples was identified by IR spectroscopy. The IR spectra of PSC and PSAC samples are shown in Fig. 1(C). The broad peak at  $3,424\text{ cm}^{-1}$  is identified as O-H and N-H stretching vibrations of hydroxyl, amine groups and absorbed water molecules in as-obtained carbon powders. The band at  $1,640\text{ cm}^{-1}$  in PSAC sample is ascribed to C=O stretching mode. The weak and wide bands between  $1,330$  to  $940\text{ cm}^{-1}$  are observed as the response of C-O stretching vibration [18].

### 4. Scanning Electron Microscopy (SEM)

The morphological information of PSC and PSAC materials was obtained by SEM. Fig. 1(D) a) and b) depict the SEM images of synthesized PSC and PSAC samples. The PSC shows stacked debris-like morphology with almost non-porous nature. The PSAC sample exhibits porous structure due to activation. The average pore diameter and height of PSC and PSAC samples are observed around  $2.40$  and  $4.31\text{ }\mu\text{m}$ , respectively. This porous nature of carbon is beneficial to improve the electrochemical performance due to increased surface area [19].

### 5. Brunauer Emmet Teller (BET)

The specific surface area of (SSA) carbons was calculated by applying Brunauer-Emmet-Teller (BET) method, and pore size dis-

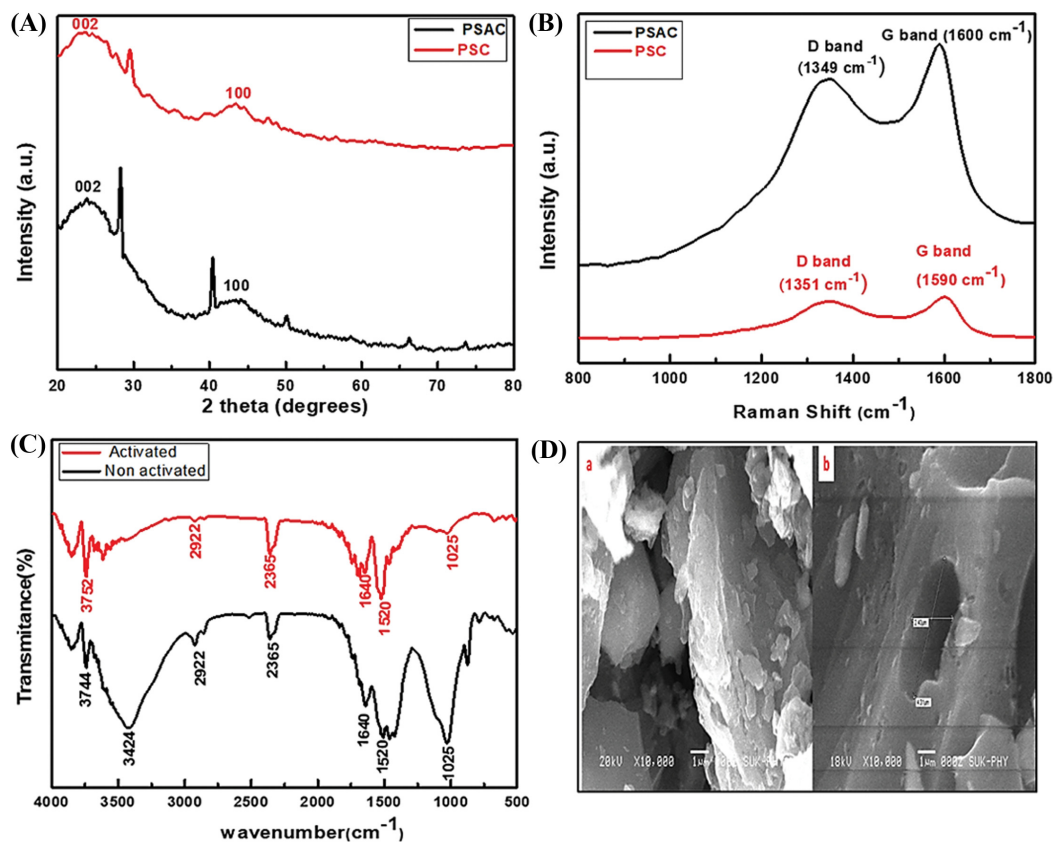


Fig. 1. (A) XRD patterns of PSC and PSAC material, (B) Raman spectra of PSC and PSAC material, (C) IR spectra of activated and non-activated PSC, and (D) SEM images of a) PSC and b) PSAC.

tribution of PSC and PSAC samples was obtained by Barret- Joyner-Halenda (BJH) method [20]. Fig. S1 shows adsorption and desorption curves of both samples and it is classified as a type IV isotherm. The BET surface areas of PSC and PSAC were found to be  $21.766 \text{ m}^2 \text{ g}^{-1}$  and  $240 \text{ m}^2 \text{ g}^{-1}$ , respectively. The sample PSAC exhibits the higher SSA and smallest particle size as compared to PSC sample. In the BJH analysis pore size distributions of 2.48 and 3.32 nm for PSC and PSAC samples were observed [19].

## 6. Electrochemical Testing

Fig. 2(a) illustrates cyclic voltammograms of PSAC electrode. The

PSAC material has retained an EDLC behavior as the scan rate increased from 10 to  $100 \text{ mV s}^{-1}$  between 0 to  $-1 \text{ V}$ . The maximum specific capacitance value obtained from CV is  $517.54 \text{ F g}^{-1}$  at  $10 \text{ mV s}^{-1}$ . The measurement of charge-discharge time of the electrode was recorded by GCD cycles. Fig. 2(b) depicts the GCD cycles of PSAC material at various current densities ranging from  $1 \text{ mA cm}^{-2}$  to  $10 \text{ mA cm}^{-2}$ . The maximum specific capacitance calculated from GCD is  $255.06 \text{ F g}^{-1}$  at  $1 \text{ mA cm}^{-2}$ . It shows excellent specific energy and specific power of the PSAC material, i.e., about  $35.42 \text{ Wh kg}^{-1}$  at  $645.16 \text{ W kg}^{-1}$ . The specific capacitance val-

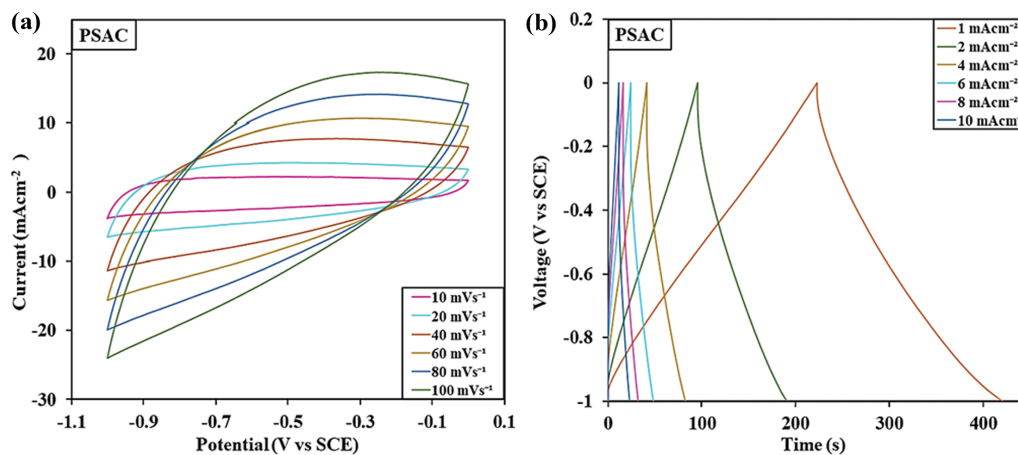


Fig. 2. (a) The cyclic voltammograms of PSAC material at different scan rates. (b) The Galvanic charge-discharge cycles of PSAC material at different current densities.

Table 1. The specific capacitance values at different scan rates and current densities.

Material	Scan rate ( $\text{mV s}^{-1}$ )	Specific capacitance form CV ( $\text{F g}^{-1}$ )	Current density ( $\text{mA cm}^{-2}$ )	Specific capacitance form GCD ( $\text{F g}^{-1}$ )
PSAC	10	517.54	1	255.06
	20	467.57	2	247.66
	40	400.21	4	212.34
	60	351.98	6	188.28
	80	334.94	8	166.50
	100	315.50	10	147.74

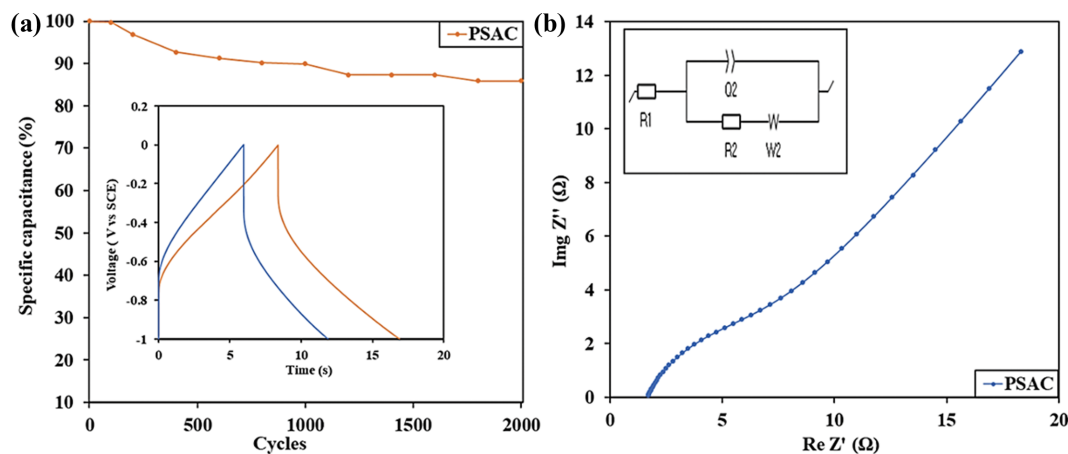


Fig. 3. (a) Cyclic stability of PSAC material up to 2000 cycles. (b) Nyquist plot and circuit fitting for PSAC material.

ues at different scan rates and current densities are listed in Table 1.

The graph in Fig. 3(a) indicates cyclic stability of PSAC material over 2000 cycles. Cycle studies were carried out by using GCD tests in the potential range  $-1$  V to  $0$  V at  $10 \text{ mA cm}^{-2}$  current density. It has shown 85.71% stability, i.e., only 14.29% deterioration in specific capacitance value.

The fundamental nature of SC is determined by using electrochemical impedance spectroscopy (EIS). Fig. 3(b) shows the Nyquist plot and circuit fitting of PSAC material. The frequency range of EIS measured is  $10 \text{ mHz}$  to  $100 \text{ KHz}$ . The impedance of PSAC material electrode, the spectra is in a slight bend at higher frequency and spike at lower frequency. Nyquist plot contains combinations of the resistance of electrolyte ionic resistance, current collector and contact resistance between active material interface and current collector. The values of resistors (R1 and R2) are  $1.66, 6.30 \Omega$  and capacitor (Q2) is  $0.88 \times 10^{-3} \text{ F}\cdot\text{s} (\text{a}^{-1})$ , which were used for circuit fitting.

## CONCLUSION

The novel PSAC material showed excellent electrochemical properties and proved to be useful active material for use in ELDCs. This scientific advancement may pave the way for additional agricultural or food-based materials for the preparation of desired graphitic carbon materials for energy storage as well as for other relevant applications.

## COMPETING INTERESTS AND CONFLICT OF INTEREST

Authors declare that there is no any conflict of interest or known competing interests associated with this work.

## FUNDING

The authors declare that no funds, grants, or other support were received during the preparation of this manuscript.

## DATA AVAILABILITY STATEMENT

No data was used.

## DECLARATIONS

### Ethics Approval

Authors approve that the submitted work is original and has not been published elsewhere in any form or language (partially or in full).

## CONSENT FOR PUBLICATION

All authors provided their consent for the publication.

## AUTHOR CONTRIBUTIONS

**PHP:** Investigation, Methodology, Data curation and Writing -

Original Draft **SBR:** Investigation, Methodology, Data curation and Writing - Original Draft **SST:** Investigation, Methodology, Data curation and Writing - Original Draft **TDD:** Resources **SAJ:** Conceptualization, Supervision, Resources and Writing - Review & Editing, Project Administration.

## SUPPORTING INFORMATION

Additional information as noted in the text. This information is available via the Internet at <http://www.springer.com/chemistry/journal/11814>.

## REFERENCES

1. E. Lim, J. Chun, C. Jo and J. Hwang, *Korean J. Chem. Eng.*, **38**, 227 (2021).
2. T. S. Bhat, S. A. Jadhav, S. A. Bknalkar, S. S. Patil and P. S. Patil, *Inorg. Chem. Commun.*, **141**, 109493 (2022).
3. P. H. Patil, V. V. Kulkarni, T. D. Dongale and S. A. Jadhav, *J. Compos. Sci.*, **7**, 167 (2023).
4. E. Dhandapani, S. Thangarasu, S. Ramesh, K. Ramesh, R. Vasudevan and N. Duraisamy, *J. Energy Storage*, **52**, 104937 (2022).
5. P. H. Patil, V. V. Kulkarni and S. A. Jadhav, *J. Compos. Sci.*, **6**, 363 (2022).
6. Md. A. Aziz, S. S. Shah, S. M. A. Nayem, M. N. Shaikh, A. S. Hakeem and I. A. Bakare, *J. Energy Storage*, **50**, 104278 (2022).
7. Y. Xi, Z. Xiao, H. Lv, H. Sun, X. Wang, Z. Zhao, S. Zhai and Q. An, *Diam. Relat. Mater.*, **128**, 109219 (2022).
8. L. Liu, X. An, Z. Tian, G. Yang, S. Nie, Z. Shang, H. Cao, Z. Cheng, S. Wang, H. Liu and Y. Ni, *Ind. Crops Prod.*, **187**, 115457 (2022).
9. B. Xing, C. Zhang, Q. Liu, C. Zhang, G. Huang, H. Guo, J. Cao, Y. Cao, J. Yu and Z. Chen, *J. Alloys Compd.*, **795**, 91 (2019).
10. R. A. Geioushy, S. Y. Attia, S. G. Mohamed, H. Li and O. A. Fouad, *J. Energy Storage*, **48**, 104034 (2022).
11. D.-Y. Kim, C.-H. Ma, Y. Jang, S. Radhakrishnan, T. H. Ko and B.-S. Kim, *Colloids Surf. A: Physicochem. Eng. Aspects*, **652**, 129785 (2022).
12. A. Shetty, V. Molahalli, A. Sharma and G. Hegde, *Catalysts*, **13**, 20 (2022).
13. G. Stella Mary, P. Sugumaran, S. Niveditha, B. Ramalakshmi, P. Ravichandran and S. Seshadri, *Int. J. Recycl. Org. Waste Agricult.*, **5**, 43 (2016).
14. X. Zhu, S. Yu, K. Xu, Y. Zhang, L. Zhang, G. Lou, Y. Wu, E. Zhu, H. Chen, Z. Shen, B. Bao and S. Fu, *Chem. Eng. Sci.*, **181**, 36 (2018).
15. M. A. El-Nemr, A. El Nemr, M. A. Hassaan, S. Ragab, L. Tedone, G. De Mastro and A. Pantaleo, *Molecules*, **27**, 4840 (2022).
16. B. Wang, L. Ji, Y. Yu, N. Wang, J. Wang and J. Zhao, *Electrochim. Acta*, **309**, 34 (2019).
17. S. Ahmed, A. Ahmed and M. Rafat, *Surf. Coat. Technol.*, **349**, 242 (2018).
18. F. O. Ochai-Ejeh, A. Bello, J. Dangbegnon, A. A. Khaleed, M. J. Madito, F. Bazegar and N. Manyala, *J. Mater. Sci.*, **52**, 10600 (2017).
19. N. Manyala, A. Bello, F. Barzegar, A. A. Khaleed, D. Y. Momodu and J. K. Dangbegnon, *Mater. Chem. Phys.*, **182**, 139 (2016).
20. S. A. Jadhav, R. Nisticò, G. Magnacca and D. Scalarone, *RSC Adv.*, **8**, 1246 (2018).

## Supporting Information

### Synthesis of graphitic carbon from *Pisum sativum* for supercapacitor applications

Pranoti H. Patil\*, Suchitra B. Ravan\*, Saurabh S. Thoravat\*, Tukaram D. Dongale\*\*, and Sushilkumar A. Jadhav\*<sup>†</sup>

\*School of Nanoscience and Technology, Shivaji University, Kolhapur 416004, Maharashtra, India

\*\*Computational Electronics and Nanoscience Research Laboratory, School of Nanoscience and Technology, Shivaji University, Kolhapur 416004, Maharashtra, India

(Received 19 April 2023 • Revised 30 May 2023 • Accepted 29 June 2023)

#### Chemicals and Reagents

Potassium hydroxide (KOH) was obtained from Molychem. Ltd., carbon black was obtained from SRL chem. Ltd., Polyvinylidene fluoride (PVDF) were obtained from Alfa Aesar, *N*-methyl pyrrolidone (NMP) was obtained from sigma Aldrich, Ethanol was obtained from Sd Fine Chem. Co. Ltd., Dry Peas and deionized water was used for the preparation of all solutions.

#### Instruments and Methods

Dry *Pisum sativum* derived carbon (PSC) and activated carbon (PSAC) were characterized by different characterization techniques. The crystal structures of PSC and PSAC samples were characterized by X-ray diffraction spectra and registered on Bruker D2 Phaser diffractometer using 5 s/scan speed. The  $2\theta$  value ranged from  $20^\circ$ - $80^\circ$  with  $\text{CuK}\alpha$  radiation ( $1.5405 \text{ \AA}$ , 30 kV, 10 mA). The attenuated total reflectance Fourier transform infrared (FTIR) spectra were recorded with Perkin Elmer spectrometer operated at room temperature ( $25 \pm 1^\circ \text{C}$ ) with nominal resolution of the detector of  $2 \text{ cm}^{-1}$ . An advanced ATR baseline correction was applied to all spectra in the range of  $4,000$  to  $600 \text{ cm}^{-1}$ . The surface morphology of PSC and PSAC samples was analysed by JEOL JSM-6360 scanning electron microscope (SEM) at an acceleration voltage of 20 kV. The BET specific surface area, total pore volume and pore size distribution of the as-prepared samples were characterized by  $\text{N}_2$  sorption

measurements on a Quantachrome autosorb automated gas sorption system. The electrochemical performance of the as-prepared electrodes was performed on Biologic VSP3 electrochemical workstation using a three-electrode testing system.

#### Formulas

The specific capacitance, energy density, power density and stability of prepared electrodes were calculated from the cyclic voltammetry and galvanostatic charge-discharge measurement using following formulas.

$$C_{sp} = \frac{1}{m \times (V_f - V_i) \times v} \int_{V_i}^{V_f} I(V) dv \dots \text{from CV} \quad (1)$$

$$C_{sp} = \frac{I \Delta t}{m \Delta V} \dots \dots \dots \text{From GCD} \quad (2)$$

$$E_{max} = \frac{0.5cv^2}{3.6} \quad (3)$$

$$P_{max} = \frac{3,600 \times E}{\Delta t} \quad (4)$$

Where,  $I$  is the current (A),  $m$  is the total mass deposited on electrodes (g),  $\Delta t$  is the discharge time (s), and  $\Delta V$  is the applied potential (V) [23].

#### Porosimetry (Nitrogen Adsorption Desorption)

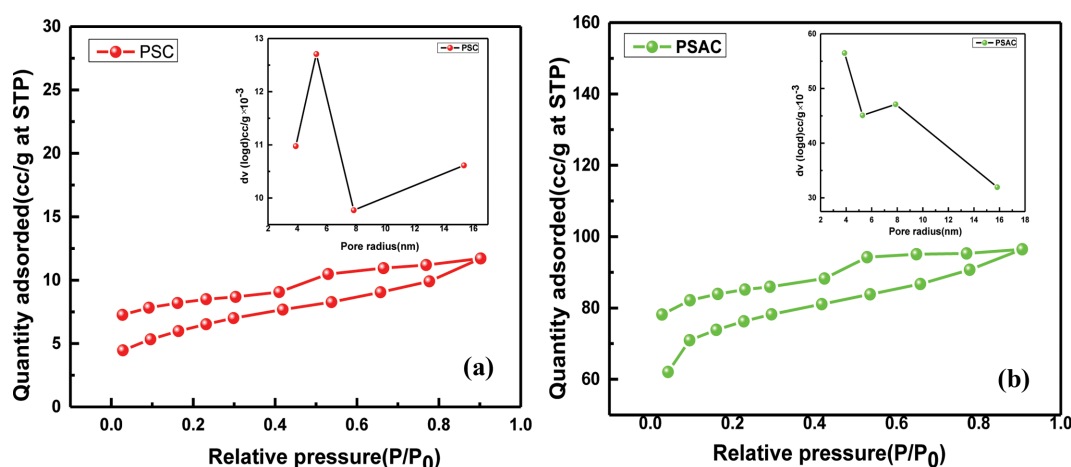


Fig. S1. (a) Shows the  $\text{N}_2$  adsorption-desorption isotherms of PSC and PSAC material, (b) isotherms using BJH method shows the pore size distribution of PSC and PSAC material calculated from the adsorption.